Time-dependent correlation functions in a one-dimensional asymmetric exclusion process

Gunter Schütz
Department of Physics, Weizmann Institute, Rehovot 76100, Israel
(Received 22 January 1993)

We continue our studies [J. Stat. Phys. **71**, 485 (1993)] of a one-dimensional anisotropic exclusion process with parallel dynamics describing particles moving to the right on a chain of L sites. Instead of considering periodic boundary conditions with a defect, as in our studies, we study open boundary conditions with injection of particles with rate α at the origin and absorption of particles with rate β at the boundary. We construct the steady state and compute the density profile as a function of α and β. In the large-L limit we find a high-density phase ($\alpha > \beta$) and a low-density phase ($\alpha < \beta$). In both phases, the density distribution along the chain approaches its respective constant bulk value exponentially on a length scale ξ. They are separated by a phase-transition line where ξ diverges and where the density increases linearly with the distance from the origin. Furthermore, we present exact expressions for all equal-time n-point density correlation functions and for the time-dependent two-point function in the steady state. We compare our results with predictions from local dynamical scaling and discuss some conjectures for other exclusion models.

PACS number(s): 05.40.+j, 05.70.Ln, 64.60.Ht

I. INTRODUCTION

We study a one-dimensional totally asymmetric exclusion model where particles are injected stochastically at the origin of a chain of L sites, move to the right according to rules defined below and are removed at its end, again according to stochastic rules. Each site of the chain can be occupied by at most one particle. Among the interesting features of such exclusion models is the occurrence of various types of phase transitions which arise from the interplay of the bulk dynamics with the boundary conditions [1–5] and their close relationship to vertex models [6], growth models [7], and, in the continuum limit, to the Kardar-Parisi-Zhang (KPZ) equation [8] and the noisy Burger's equation.

Exclusion models can be divided into four classes according to the dynamics (*parallel* or *sequential*) and the boundary conditions [*periodic* with conservation of the number of particles and (possibly) a defect or *open* with injection and absorption of particles]. According to this classification we call them *p-p* models (parallel, periodic), *p-o* models (parallel, open), *s-p* models (sequential, periodic), and *s-o* models (sequential, open). A *s-p* model with a defect has been studied numerically by Janowsky and Lebowitz [3], without a defect it was solved by a Bethe ansatz by Gwa and Spohn [9]. The *s-o* model was studied numerically by Krug [2]; later the exact solution with the full phase diagram was found [4, 5]. In addition to the density profile all equal-time n-point density correlation functions in the steady state were determined [10]. Previously we solved a *p-p* model with a defect [1] with Bethe ansatz methods and obtained the density profile and the equal-time two-point correlation function in the steady state.

Here we discuss the *p-o* model with the same parallel dynamics as in [1] but with open boundary conditions where particles are injected at the origin with a rate α and are removed at the (right) boundary with rate β. The bulk dynamics of our model are deterministic and defined as follows: Each site x on the ring ($1 \le x \le L$) is either occupied [$\tau_x(t) = 1$] or empty [$\tau_x(t) = 0$] at time t. The time evolution consists of two half time steps. In the first half step we divide the chain with L sites (L even) into pairs of sites (2,3), (4,5), ..., (L, 1). If both sites in a pair are occupied or empty or if site $2x$ is empty and site $2x+1$ occupied, they remain so at the intermediate time $t' = t + 1/2$. If site $2x$ is occupied and site $2x+1$ empty, then the particle moves with probability 1 to site $2x+1$, i.e.,

$$\begin{aligned} \tau_{2x}(t') &= \tau_{2x}(t)\tau_{2x+1}(t), \\ \tau_{2x+1}(t') &= \tau_{2x}(t) + \tau_{2x+1}(t) - \tau_{2x}(t)\tau_{2x+1}(t). \end{aligned} \tag{1}$$

These rules are applied in parallel to all pairs except the pair (L,1). In this pair representing the boundary (site L) and the origin (site 1), respectively, particles are absorbed and injected according to the following stochastic rules. If site 1 was empty at time t then it remains so with probability $1-\alpha$ and becomes occupied with probability α at time t'. If site 1 was occupied at time t then it remains occupied with probability 1. These two rules are independent of the occupation of site L. On the other hand, if site L was occupied at time t it remains so with probability $1-\beta$ and becomes empty with probability β. If site L was empty, it remains empty with probability 1. These two rules are independent of the occupation of site 1. This means that in contrast to the models with sequential dynamics studied in Refs. [2, 4, 5, 10] simultaneous injection and absorption is allowed with probability $\alpha\beta$. We have

$$\begin{aligned} \tau_1(t') &= 1 \text{ with probability } \tau_1(t) + \alpha(1-\tau_1(t)) , \\ \tau_1(t') &= 0 \text{ with probability } (1-\alpha)(1-\tau_1(t)) , \\ \tau_L(t') &= 1 \text{ with probability } (1-\beta)\tau_L(t), \\ \tau_L(t') &= 0 \text{ with probability } 1-(1-\beta)\tau_L(t). \end{aligned} \tag{2}$$

In the second half step $t+1/2 \rightarrow t+1$ the pairing is shifted by one lattice unit such that the pairs are now (1,2), (3,4), ..., $(L-1, L)$. Here rules (1) are applied in *all* these pairs, there is no injection, and absorption in the second half time step. Note that we reverse the order of the choice of pairs as compared to [1]. There the pairs were chosen as (1,2), (3,4), ... in the first half time step.

In the mapping of Ref. [6] this model is equivalent to a two-dimensional four-vertex model in thermal equilibrium with a defect line where other vertices, not belonging to the group defining the six-vertex model or eight-vertex model, have nonvanishing Boltzmann weights. The two steps describing the motion of particles define the diagonal-to-diagonal transfer matrix $T(\alpha,\beta)$ in the vertex model (see the Appendix). The pairing is chosen as in [6] but the hopping probabilities are different.

For the Bethe ansatz solution of the *p-p* model with a defect [1] the conservation of the number of particles was crucial and we cannot repeat the calculation here, where the particle number is not conserved. However, since we are only interested in the steady state we can construct the steady state explicitly for small lattices and then try to guess its general form for arbitrary length L. This method was successfully applied in Refs. [4] and [5] and led to exact expressions for the particle current and the density profile for arbitrary values of the injection and absorption rates. Only after guesswork produced the correct results, were they actually proven (see also [10]). It turns out that also here we can estimate rules for the construction of the steady state. Instead of proving them we verified our conjecture for lattices of up to 14 sites. In the same way we guessed and verified expressions for the density profile (the one-point density correlator $\langle \tau_x \rangle$ in the steady state) Eq. (18) and the equal-time n-point density correlation function (30). The simple form of these correlation functions then allowed for a conjecture of the time-dependent two-point function $\langle \tau_x T^t \tau_y \rangle$ (37)–(41). [In this expression T^t denotes the tth power of the transfer matrix $T(\alpha,\beta)$]. The mapping to the vertex model allows for an independent verification of this result.

Among other things the time-dependent two-point function is of interest for the study of local dynamical scaling in the absence of translational invariance. Dynamical scaling in a (1+1)-dimensional system with translational invariance both in space and time direction implies that the two-point function $G(r,t)$ behaves under a global rescaling λ of the space and time coordinates as [11]

$$G(\lambda r, \lambda^z t) = \lambda^{-2x} G(r,t) \quad . \tag{3}$$

In this expression r denotes the distance in space direction, t is the distance in time direction, z is the dynamic critical exponent, and x is the scaling dimension. From (3) it follows that the correlation function has the form

$$G(r,t) = t^{-2x/z}\, \Phi(\tfrac{r^z}{t}) \tag{4}$$

with the scaling function Φ which is not determined by global dynamical scaling. By extending the concept of global rescaling to local, space-time-dependent rescaling, it has been shown that for the special case $z=2$ the correlation function $G(r,t)$ is of the form [12, 13]

$$G(r,t) = a t^{-x}\, \mathrm{e}^{-\frac{br^2}{2t}} \tag{5}$$

with some constants a and b, i.e., $\Phi(r^2/t) = a \exp(-br^2/t)$. The (connected) density correlation function in the probabilistic symmetric *p-p* model without the defect computed in [6] is indeed of this form with critical exponent $x = 1/2$. Since we study the steady state we have translational invariance in the time direction, but due to the open boundary conditions translational invariance is broken in space direction. In Sec. V we show that the form of $\langle \tau_x T^t \tau_y \rangle$ for large L on the critical line $\alpha = \beta$ and in the scaling regime close to it resembles (5) with $x = 0$ (Sec. V), i.e., one has $z = 2$, but there are additional pieces that arise from the breaking of translational invariance.

The paper is organized as follows. In Sec. II we present our conjectured rules for the construction of the steady state and exact expressions for the current and the density profile. In Sec. III we study the limit of large L and derive the phase diagram. In Sec. IV we present expressions for the equal-time n-point density correlation function. They turn out to be reducible to a sum of one-point functions through associative fusion rules of the density operators. In particular we study the two-point function in the scaling regime. In Sec. V we compute the time-dependent two-point correlator. Again we put our emphasis on the vicinity to the phase-transition line. In Sec. VI we summarize our main results and discuss our results in the context of other exclusion models. In the Appendix we discuss the mapping to a two-dimensional vertex model.

II. CONSTRUCTION OF THE STEADY STATE

Before we discuss the construction of the steady state we introduce some useful notations. In anticipation of the correspondence of the model to a vertex model discussed in Refs. [1, 6] and in the Appendix we denote a state of the system with N particles placed on sites $x_1, \ldots, x_N$ and holes everywhere else by $|\, x_1, \ldots, x_N \,\rangle$. The transfer matrix $T(\alpha,\beta)$ (A1) acting on the space of states spanned by these vectors acts as time evolution operator and encodes the dynamics and the boundary conditions of the system as defined by Eqs. (1) and (2). The steady state is the (right) eigenvector with eigenvalue 1 of the transfer matrix $T(\alpha,\beta)$ and we denote it by

$$|\, 1\,\rangle = \sum_{N=0}^{L} \sum_{\{x\}} \Psi_N(x_1,\ldots,x_N) |\, x_1,\ldots,x_N\,\rangle \quad . \tag{6}$$

Here the N-particle "wave function" $\Psi_N(x_1,\ldots,x_N)$ is the unnormalized probability of finding the particular configuration $|\, x_1,\ldots,x_N\,\rangle$ of N particles in the steady state. We denote the state with no particles by $|\,\rangle$ and the corresponding wave function by Ψ_0. The summation runs over all states of N particles ($0 \leq N \leq L$) and all possible configurations $\{x\} = \{x_1,\ldots,x_N\}$ and one has $T(\alpha,\beta)|\,1\,\rangle = |\,1\,\rangle$. The normalized probabilities are given by

$$p_N(x_1,\ldots,x_N)=\Psi_N(x_1,\ldots,x_N)/Z_L \tag{7}$$

with

$$Z_L=\sum_{N=0}^{L}\sum_{\{x\}}\Psi_N(x_1,\ldots,x_N) \ . \tag{8}$$

The transfer matrix $T(\alpha,\beta)$ has a left eigenvector $\langle\, 1\,|$ with eigenvalue 1 given by

$$\langle\, 1\,| = \sum_{N=0}^{L}\sum_{\{x\}}\langle\, x_1,\ldots,x_N\,| \ , \tag{9}$$

where $\langle\, x_1,\ldots,x_N\,|$ is the transposed vector to $|\, x_1,\ldots,x_N\,\rangle$. Defining a scalar product in the standard way (i.e., $\langle\, x_1,\ldots,x_N\,|y_1,\ldots,y_M\,\rangle = 1$ if the sets $\{x\}$ and $\{y\}$ are identical and 0 otherwise), one can write Z_L as the scalar product $Z_L=\langle\, 1\,|\,1\,\rangle$.

Furthermore, we denote the projection operator on particles on site x by τ_x:

$$\tau_x|\, x_1,\ldots,x_N\,\rangle=\begin{cases}|\, x_1,\ldots,x_N\,\rangle & \text{if } x\in\{x_1,\ldots,x_N\}\\ 0 & \text{otherwise.}\end{cases} \tag{10}$$

The projector on holes is $\sigma_x=1-\tau_x$. Expectation values $\langle\, \tau_{x_1}\cdots\tau_{x_k}\,\rangle$ of the operators τ_x and their products in the steady state can be conveniently written in the form

$$\langle\, \tau_{x_1}\cdots\tau_{x_k}\,\rangle=\langle\, 1\,|\tau_{x_1}\cdots\tau_{x_k}|\,1\,\rangle/Z_L \ . \tag{11}$$

Taking the scalar product with the left eigenvector $\langle\, 1\,|$ and dividing by the normalization sum Z_L is equivalent to a summation over all probabilities $p_N(y_1,\ldots,y_N)$ with $\{x_1,\ldots,x_k\}\in\{y_1,\ldots,y_N\}$. This is the definition of an expectation value in the steady state.

The particle current j is a conserved quantity in the bulk since only the origin and the boundary act as a source or sink of particles. It is given by the correlator [1] [see (A6)]

$$j=\langle\, \tau_{2x}\sigma_{2x+1}\,\rangle \ . \tag{12}$$

Now we discuss the construction of the steady state. In [1] we derived the important result that for the deterministic dynamics defined by (1) one has

$$\tau_{2x-1}\sigma_{2y}|\,\Lambda\,\rangle=0 \tag{13}$$

for $1\le x\le L/2$ and $x\le y\le L/2$ and *any* right eigenvector $|\,\Lambda\,\rangle$ of the transfer matrix. This simplifies the construction of the steady state considerably: If in a state $|\, x_1,\ldots,x_N\,\rangle$ one of the x_i is odd, then it has a nonvanishing weight $\Psi_N(x_1,\ldots,x_N)$ only if *all* even x_j with $x_i<x_j\le L$ are also contained in the set $\{x_1,\ldots,x_N\}$.

Using this it is easy to construct the steady state explicitly for small L. We discovered that the unnormalized probabilities $\Psi_N^{(L+2)}(x_1,\ldots,x_N)$ in the chain with $L+2$ sites can be constructed recursively out those of the chain with L sites according to the following rules.

Rule 1: $(0\le N\le L,\text{all }\{x\})$,

$$\Psi_N^{(L+2)}(x_1+2,x_2+2,\ldots,x_N+2)=\beta^2(1-\alpha)\Psi_N^{(L)}(x_1,x_2,\ldots,x_N).$$

Rule 2: $(0\le N\le L,\text{all }\{x\})$,

$$\Psi_{N+2}^{(L+2)}(2,x_1,\ldots,x_{N-1},L+1,L+2)=\alpha^2(1-\beta)\Psi_N^{(L)}(2,x_1,\ldots,x_{N-1}).$$

Rule 3: $(0\le N\le L/2,\{x_1,\ldots,x_{L/2}\}\neq\{2,4,6,\ldots,L-2,L\})$,

$$\Psi_{N+1}^{(L+2)}(2,x_1+2,x_2+2,\ldots,x_N+2)=\alpha\beta^2\Psi_N^{(L)}(x_1,x_2,\ldots,x_N). \tag{14}$$

Rule 4: $(L/2\le N\le L,\{x_1,\ldots,x_{L/2}\}\neq\{2,4,6,\ldots,L-2,L\})$,

$$\Psi_{N+1}^{(L+2)}(x_1,x_2,\ldots,x_N,L+2)=\alpha^2\beta\Psi_N^{(L)}(x_1,x_2,\ldots,x_N).$$

Rule 5: $(\{x_1,\ldots,x_{L/2}\}=\{2,4,6,\ldots,L-2,L\})$,

$$\Psi_{L/2+1}^{(L+2)}(2,4,\ldots,L,L+2)=\alpha\beta(\alpha+\beta)\Psi_{L/2}^{(L)}(2,4,\ldots,L)-(\alpha\beta)^{L/2+3}.$$

These rules together with (13) and the initial conditions

$$\Psi_0^{(2)}=\beta^2(1-\alpha),\quad \Psi_1^{(2)}(2)=\alpha\beta, \qquad \Psi_2^{(2)}(1,2)=\alpha^2(1-\beta) \tag{15}$$

define recursively all quantities $\Psi_N^{(L+2)}(x_1,\ldots,x_N)$ in the chain with $L+2$ sites.

Based on these rules we constructed the steady state up to $L=14$ and verified that it has indeed eigenvalue 1 of $T(\alpha,\beta)$. In a next step we computed the sum over all $\Psi_N(x_1,\ldots,x_N)$ and concluded that the normalization Z_L (8) is given by

$$\begin{aligned}Z_L&=(1-\beta)\alpha^L\sum_{k=0}^{L/2-1}\left(\frac{\beta}{\alpha}\right)^k+(1-\alpha)\beta^L\sum_{k=0}^{L/2-1}\left(\frac{\alpha}{\beta}\right)^k+(\alpha\beta)^{L/2}\\&=\begin{cases}\dfrac{(1-\beta)\alpha^{L+1}-(1-\alpha)\beta^{L+1}}{\alpha-\beta}, & \alpha\neq\beta\\ \alpha^L(1+L(1-\alpha)), & \alpha=\beta.\end{cases}\end{aligned} \tag{16}$$

This result was again checked explicitly up to $L=14$.

Going one step further we consider the average density $\langle\, \tau_x\,\rangle$ at site x defined by (11). We found the following exact expressions for the even and odd sublattices, respectively:

$$Z_L\langle \tau_{2x} \rangle = \begin{cases} (1-\beta)\alpha^L \sum_{k=0}^{2x-1} \left(\frac{\beta}{\alpha}\right)^k + (1-\beta)\alpha^{L+1} \sum_{k=2x}^{L} \left(\frac{\beta}{\alpha}\right)^k + (\alpha\beta)^{L+1}, & \alpha \neq \beta \\ \alpha^{L+1}(1+L(1-\alpha)) + 2x\alpha^L(1-\alpha)^2, & \alpha=\beta, \end{cases}$$

$$Z_L\langle \tau_{2x-1} \rangle = \begin{cases} (1-\beta)^2\alpha^L \sum_{k=0}^{2x-3} \left(\frac{\beta}{\alpha}\right)^k + (1-\beta)\alpha^{L+2-2x}\beta^{2x-2}, & \alpha \neq \beta \\ \alpha^{L+1}(1-\alpha) + (2x-1)\alpha^L(1-\alpha)^2, & \alpha=\beta. \end{cases} \tag{17}$$

Performing the summations and dividing by 2 we arrive at the main result of this section,

$$\langle \tau_{2x} \rangle = \begin{cases} \alpha + (1-\alpha)\frac{1-(\frac{\beta}{\alpha})^{2x}}{1-\frac{1-\alpha}{1-\beta}(\frac{\beta}{\alpha})^{L+1}}, & \alpha\neq\beta \\ \alpha + (1-\alpha)^2\frac{2x}{1+L(1-\alpha)}, & \alpha=\beta, \end{cases}$$

$$\langle \tau_{2x-1} \rangle = \begin{cases} (1-\beta)\frac{1-\frac{1-\alpha}{1-\beta}(\frac{\beta}{\alpha})^{2x-1}}{1-\frac{1-\alpha}{1-\beta}(\frac{\beta}{\alpha})^{L+1}}, & \alpha\neq\beta \\ (1-\alpha)^2\frac{2x}{1+L(1-\alpha)} + \frac{\alpha(1-\alpha)}{1+L(1-\alpha)}, \\ \alpha=\beta. \end{cases} \tag{18}$$

The anisotropy between the even and odd sublattices is a consequence of the parallel updating mechanism [1] and is related to the net particle current (12) for which we found (again, by direct evaluation on small lattices and estimating the general form for arbitrary L)

$$j = \begin{cases} \alpha - \frac{\alpha-\beta}{1-\frac{1-\alpha}{1-\beta}(\frac{\beta}{\alpha})^{L+1}}, & \alpha\neq\beta \\ \alpha - \frac{\alpha(1-\alpha)}{1+L(1-\alpha)}, & \alpha=\beta. \end{cases} \tag{19}$$

The fact that this quantitity is independent on x as it should be is an additional nontrivial check for our conjectures.

Finally, note that by the definition of the model there is the particle-hole symmetry (A5): Changing particles into holes, reflecting site x into site $L+1-x$, and exchanging α and β leaves the system invariant. All our results are indeed invariant under this operation.

III. THE PHASE DIAGRAM

From Eqs. (18) one realizes that the system changes its behavior if $\alpha=\beta$. The average densities on the even and odd sublattices

$$\rho^{(\text{even})} = \frac{2}{L}\sum_{x=1}^{L/2}\langle \tau_{2x} \rangle, \quad \rho^{(\text{odd})} = \frac{2}{L}\sum_{x=1}^{L/2}\langle \tau_{2x-1} \rangle \tag{20}$$

have a discontinuity in the thermodynamic limit $L\to\infty$ at $\alpha=\beta\neq 0,1$. If α or β is either 0 or 1 the system is trivial in the sense that the density profile is exactly constant (even in finite systems) and all correlation functions can be obtained without any calculation (see the Appendix). Therefore we exclude these cases from our discussion. One finds from (18)

$$\rho^{(\text{even})} = \begin{cases} \alpha, & \alpha<\beta \\ 1, & \alpha>\beta, \end{cases} \qquad \rho^{(\text{odd})} = \begin{cases} 0, & \alpha<\beta \\ 1-\beta, & \alpha>\beta. \end{cases} \tag{21}$$

On the phase-transition line $\alpha=\beta$ one obtains $\rho^{(\text{even})} = (1+\alpha)/2$ and $\rho^{(\text{odd})} = (1-\alpha)/2$, respectively. For $\alpha<\beta$ (more particles are absorbed than injected) the system is in a low-density phase with total average density $\rho = \frac{1}{2}(\rho^{(\text{even})}+\rho^{(\text{odd})}) = \alpha/2 < \frac{1}{2}$, while for $\alpha>\beta$ it is in a high-density phase with $\rho = 1-\beta/2 > \frac{1}{2}$ (Fig. 1).

In the thermodynamic limit $L\to\infty$ the current j (19) is given by

$$j = \min(\alpha,\beta) \ . \tag{22}$$

There is no discontinuity at $\alpha=\beta$ in the current, but its first derivatives with respect to α and β are discontinous. The discontinuity of ρ at the phase-transition line $\alpha=\beta$ and Eq. (22) reminds us of the *s-o* model [4, 5, 10]. In

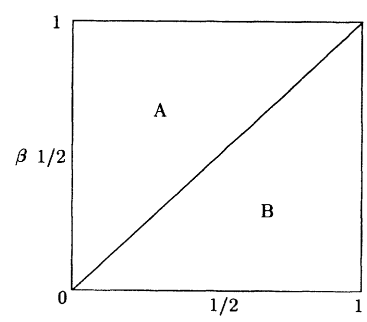

FIG. 1. Phase diagram of the model in the α-β plane. Region A is the low-density phase and region B the high-density phase. The phases are separated by the curve $\alpha=\beta$.

this model in the region $\alpha, \beta < 1/2$ the phase diagram shows a low-density phase $A_{\rm I}$ and a high-density phase $B_{\rm I}$ separated by a phase-transition line at $\alpha = \beta$ [5]. Also in this model the density and the first derivatives of the current with respect to the injection and absorption rates α and β have a discontinuity at the phase-transition line.

In terms of the sublattice densities the current j is given by $j = \rho^{(\rm even)} - \rho^{(\rm odd)}$ for all α, β. In terms of the total average density ρ the current satisfies $j = 2\rho$ if $\rho < 1/2$ (low-density phase) and $j = 2(1-\rho)$ if $\rho > 1/2$ (high-density phase). These are the same relations as in the p-p model in the respective phases [1].

Now we turn to a discussion of the density profile. We first study the case $\alpha < \beta$ and $L \to \infty$. Defining the decay length ξ by

$$\xi^{-1} = \ln \frac{\beta}{\alpha}, \tag{23}$$

one obtains from (18) the density profile up to corrections of order $\exp(-L/\xi)$

$$\begin{aligned} \langle \tau_{2x} \rangle &= \alpha + (1-\beta) e^{-(L+1-2x)/\xi}, \\ \langle \tau_{2x-1} \rangle &= (1-\beta) e^{-(L+2-2x)/\xi} \ . \end{aligned} \tag{24}$$

The profile decays exponentially with increasing distance from the boundary to its respective bulk values $\rho_{\rm bulk}^{(\rm even)} = \alpha$ and $\rho_{\rm bulk}^{(\rm odd)} = 0$. This is the low-density phase of the system.

In the high-density phase $\alpha > \beta$ which is related to the low-density phase by the particle-hole symmetry the profile is given by

$$\begin{aligned} \langle \tau_{2x} \rangle &= 1 - (1-\alpha) e^{-2x/\xi}, \\ \langle \tau_{2x-1} \rangle &= 1 - \beta - (1-\alpha) e^{-(2x-1)/\xi} \ . \end{aligned} \tag{25}$$

The bulk densities are $\rho_{\rm bulk}^{(\rm even)} = 1$ and $\rho_{\rm bulk}^{(\rm odd)} = 1-\beta$.

On approaching the phase-transition line $\alpha = \beta$ the decay length ξ diverges. On the line the profile is linear and up to corrections of order L^{-1} given by

$$\begin{aligned} \langle \tau_{2x} \rangle &= \alpha + (1-\alpha) \frac{2x}{L}, \\ \langle \tau_{2x-1} \rangle &= (1-\alpha) \frac{2x-1}{L} \ . \end{aligned} \tag{26}$$

An explanation for the shape of the profile in the two phases and on the phase-transition line will be given in the next section.

IV. EQUAL-TIME CORRELATION FUNCTIONS

Having found exact expressions for the current and the density profile we proceed by calculating the n-point equal-time density correlation function $\langle \tau_{x_1} \cdots \tau_{x_n} \rangle$ in the steady state. Examining the two-point function for small L, we found the following *exact* relations for $1 \le x < y \le L/2$:

$$\begin{aligned} \langle \tau_{2x}\tau_{2y} \rangle &= \langle \tau_{2x} \rangle - \alpha + \alpha \langle \tau_{2y} \rangle, \\ \langle \tau_{2x}\tau_{2y-1} \rangle &= (1-\beta)(\langle \tau_{2x} \rangle - \alpha) + \alpha \langle \tau_{2y-1} \rangle, \\ \langle \tau_{2x+1}\tau_{2y} \rangle &= \langle \tau_{2x+1} \rangle, \\ \langle \tau_{2x-1}\tau_{2y-1} \rangle &= (1-\beta) \langle \tau_{2x-1} \rangle. \end{aligned} \tag{27}$$

The third of these equations is a simple consequence of (13), which indicates that whenever there is a particle on an odd lattice site then all even lattice sites to its right must be occupied as well. The important result is that the two-point is completely determined by the one-point function and some constants. Proceeding further we made the surprising observation that the n-point function can also be expressed in terms of one-point functions by repeatedly fusing products of *operators* $\tau_x \tau_y$ according to the fusion rules that are defined by (27) by omitting the averaging. This fusion can be performed in arbitrary order until one reaches the one-point level.

The fusion rules implied by Eqs. (27) can be simplified by using operators η_x defined by

$$\eta_{2x} = \frac{\tau_{2x} - \alpha}{1-\alpha}, \qquad \eta_{2x-1} = \frac{\tau_{2x-1}}{1-\beta} \tag{28}$$

instead of using the density operators τ_x. In the bulk of the high-density region both $\langle \eta_{2x} \rangle$ and $\langle \eta_{2x-1} \rangle$ take the value 1, while in the bulk of the low-density region both average values are 0. Expressing all τ_x in terms of the η_x the correlation functions (27) become

$$\langle \eta_{x_1} \eta_{x_2} \rangle = \langle \eta_{x_1} \rangle \qquad (x_2 > x_1) \ . \tag{29}$$

Fusion of n operators $\eta_{x_1} \cdots \eta_{x_n}$ gives η_{x_i} with $x_i = \min\{x_1, \ldots, x_n\}$. So the n-point correlation function is

$$\langle \eta_{x_1} \cdots \eta_{x_n} \rangle = \langle \eta_{x_i} \rangle \quad (x_i = \min\{x_1, \ldots, x_n\}) \ . \tag{30}$$

This is the main result of this section.

The form of the two-point function (29) can be understood by considering the steady state as composed of "constituent profiles" with a region of constant low density up to some point x_0 in the chain followed by a high-density region beyond this "domain wall." Such an assumption explains why the correlator (29) does not depend on x_2: In the low-density region of density α on the even sublattice and 0 on the odd sublattice the operator η_{x_1} has a vanishing expectation value and therefore the whole expression $\langle \eta_{x_1} \eta_{x_2} \rangle$ is zero if x_1 is in this region, independent of η_{x_2}. If, however, x_1 is in a region of high density, then, according to our assumption, also $x_2 > x_1$ must be in a region of high density. Thus, $\eta_{x_1} \eta_{x_2}$ again does not depend on x_2 and takes the value 1. We conclude that the product $\eta_{x_1} \eta_{x_2}$ is either 0 or 1, depending on whether x_1 is in a region of low or high density. This leads to the expression (29) for the expectation value of this product.

The average value $\langle \eta_x \rangle$ itself contains the information about the position x_0 of the domain wall. In the low-density phase the density profile decays exponentially from above to its bulk value with increasing distance from the boundary. This means that the probability of finding the domain wall also decreases exponentially with the same decay length ξ with the distance from the boundary. The domain wall is caused by particles hitting the boundary where they get stuck with probability $1-\beta$ and then cause other incoming particles to pile up and create a region of high density (Fig. 4 in the Appendix). On the other hand, in the high-density phase where the rate of injection is higher than the absorption rate the situation is reversed. Here the probability of finding the domain wall decreases exponentially with the distance from the origin. This can alternatively be explained either in terms of holes through the particle-hole symmetry or in terms of particles being piled up from the boundary over the whole system up to a point close to the origin. On the phase-transition line injection and absorption are in balance and the probability of finding the domain wall is space independent and the density profile is a linear superposition of the assumed step function constituent profiles. This leads to the observed linearly increasing average density (15).

We conclude this section by studying the two-point function in more detail in the limit $L \to \infty$. We define the equal-time connected two-point function by

$$G_c(x_1,x_2;t=0) = \langle \eta_{x_1}\eta_{x_2} \rangle - \langle \eta_{x_1} \rangle \langle \eta_{x_2} \rangle = \frac{\langle \tau_{x_1}\tau_{x_2} \rangle - \langle \tau_{x_1} \rangle\langle \tau_{x_2} \rangle}{(1-\alpha)^m(1-\beta)^n}, \tag{31}$$

where $m=2, n=0$ if both x_1 and x_2 are even, $n=2, m=0$ if both x_1 and x_2 are odd, and $m=n=1$ else.

In what follows we restrict ourselves to the case where x_1 and x_2 are both odd, the mixed correlators can be computed analogously. From (29) one obtains $G(x_1,x_2;0) = \langle \eta_{x_1} \rangle (1-\langle \eta_{x_2} \rangle)$ and inserting the expressions for the density profile (13)–(15) one obtains with $x_2 = x_1 + 2r$ $(r>0)$

$$G_c(x_1,x_2;0) = \begin{cases} A(x_2)\mathrm{e}^{-2r/\xi}, & \alpha<\beta \\ \tilde{A}(x_1)\mathrm{e}^{-2r/\xi}, & \alpha>\beta \\ \frac{x_1}{L}(1-\frac{x_1}{L}) - \frac{x_1}{L}\frac{r}{L}, & \alpha=\beta. \end{cases} \tag{32}$$

The amplitudes of the exponential decay are given by

$$\begin{aligned} A(x) &= \mathrm{e}^{-R/\xi}\left(1-\mathrm{e}^{-R/\xi}\right), \\ \tilde{A}(x) &= \frac{1-\alpha}{1-\beta}\mathrm{e}^{-x/\xi}\left(1-\frac{1-\alpha}{1-\beta}\mathrm{e}^{-x/\xi}\right), \end{aligned} \tag{33}$$

where $R = L+1-x$ measures the distance of site x from the boundary.

The decay length ξ is identical with the correlation length of the connected two-point function. On the phase-transition line the correlation function is constant for relative distances $2r \ll L$. Its amplitude depends on the position x_1 in the bulk. A similar form of the connected equal-time correlator was found in the p-p model with a defect [1].

V. TIME-DEPENDENT CORRELATION FUNCTIONS

In this section we study the time-dependent two-point correlation function in the steady state

$$G(x_1,x_2;t) = \langle \eta_{x_1} T^t \eta_{x_2} \rangle, \tag{34}$$

where T^t denotes the tth power of the transfer matrix T. Note that $t=1$ corresponds to a distance of two lattice units in time direction in the underlying vertex model (see the Appendix). We define the direction of the time evolution formally by $T^{-t}\tau_x(t_0)T^t = \tau_x(t_0+t)$, thus $G(x_1,x_2;t) = \langle \eta_{x_1}(t_0+t)\eta_{x_2}(t_0) \rangle$. The connected two-point function is defined by $G_c(x_1,x_2;t) = G(x_1,x_2;t) - \langle \eta_{x_1} \rangle \langle \eta_{x_2} \rangle$.

The standard way of computing the correlation function (34) would be the insertion of a complete set of eigenstates of T, evaluating the matrix elements $a_k(x_1) = \langle 1 | \eta_{x_1} | \Lambda_k \rangle$ and $\tilde{a}_k(x_2) = \langle \Lambda_k | \eta_{x_2} | 1 \rangle$ and summing over $a_k \tilde{a}_k \Lambda_k^t$. Since we do not know the eigenstates and eigenvalues we take the alternative route using the commutator of $[\eta_x, T^t]$. Since $\langle 1 |$ is a left eigenvector of T with eigenvalue 1 one has

$$\begin{aligned} \langle [\eta_x, T^t]\eta_{x_2} \rangle &= \langle 1 | (\eta_{x_1}T^t - T^t\eta_{x_1})\eta_{x_2} | 1 \rangle \\ &= G_c(x_1,x_2;t). \end{aligned}$$

From this one obtains $G(x_1,x_2;t)$.

First we note that from the commutation relations (A7) of τ_x with T one obtains

$$\begin{aligned} \tau_{2x-1}\,T &= T\,(1-\sigma_{2x-2}\sigma_{2x-1})\tau_{2x}\tau_{2x+1}, \\ \tau_{2x}\,T &= T\,(1-\sigma_{2x-2}\sigma_{2x-1}(1-\tau_{2x}\tau_{2x+1})). \end{aligned} \tag{35}$$

It is obvious that evaluating $\tau_x T^t$ is not an easy task. By iterating relations (35) t times not only the number of terms in the products on the right-hand side (rhs) but also the total number of such multipoint correlators increases extremely fast with t. It is only the simplicity of the multipoint correlators [see Eqs. (29) and (30)] that makes this approach promising. We restrict our discussion again to both $x_1 = 2y_1 - 1$ and $x_2 = 2y_2 - 1$ odd.

By iterating (35) t times one finds that $\tau_{2y_1-1}T^t\tau_{2y_2-1}$ is of the form

$$\begin{aligned} \tau_{2y_1-1}T^t\tau_{2y_2-1} = T^t\Big\{ & 1 - (\sigma_{2y_1-2t}\sigma_{2y_1-2t+1}\cdots) - (\sigma_{2y_1-2t+2}\sigma_{2y_1-2t+3}\cdots) - (\cdots) - (\sigma_{2y_1-2t+2k}\sigma_{2y_1-2t+2k+1}\cdots) \\ & -(\cdots) - \sigma_{2y_1-4+2t}\sigma_{2y_1-3+2t}\Big\}\tau_{2y_1-2+2t}\tau_{2y_1-1+2t}\tau_{2y_2-1}, \end{aligned} \tag{36}$$

where the ellipses denote some complicated sums of products of operators τ_y acting on sites y between $2y_1 - 2t$ and $2y_1 - 1 + 2t$. $\sigma_y = 1 - \tau_y$ denotes the projector on holes and in order to avoid boundary effects one has to choose $t < y_1 - 1$. We first discuss the correlation function outside the light cone, then on the edges of the light cone and finally in its interior.

A. Correlation function outside the light cone

We want to evaluate $\langle \tau_{2y_1-1} T^t \tau_{2y_2-1} \rangle$ with $2y_1 - 1 \geq 2y_2 - 1 + 2t$. Recalling the fusion rule $\langle \tau_{2x+1}\tau_{2y} \rangle = \langle \tau_{2x+1} \rangle$ for $y > x$ (27), one obtains $\langle \tau_{2x+1}\sigma_{2y} \rangle = 0$ for $y > x$. Since the fusion procedure is associative all terms on the rhs of (36) vanish when contracted with τ_{2y_2-1} except

$$\langle \tau_{2y_2-1}\tau_{2y_1-2+2t}\tau_{2y_1-1+2t} \rangle = \langle \tau_{2y_1-1-2t}\tau_{2y_1-2+2t}\tau_{2y_1-1+2t} \rangle.$$

Using also $\langle \tau_{2x-1}\tau_{2y-1} \rangle = (1-\beta)\langle \tau_{2x-1} \rangle$ for $y > x$ one gets

$$\langle \tau_{2y_1-1-2t}\tau_{2y_1-2+2t}\tau_{2y_1-1+2t} \rangle = (1-\beta)\langle \tau_{2y_1-1-2t} \rangle.$$

Therefore we obtain

$$G(x_1, x_2; t) = \langle \eta_{x_2} \rangle \quad (x_1, x_2 \text{ odd}, \, x_1 \geq x_2 + 2t) \ . \tag{37}$$

Now we study the correlator $\langle \tau_{2y_1-1} T^t \tau_{2y_2-1} \rangle$ with $2y_1 - 1 \leq 2y_2 - 3 - 2t$. Here the fusion of τ_{2y_1-1+2t} on the rhs of (36) with τ_{2y_2-1} yields $(1-\beta)\tau_{2y_1-1+2t}$ and by taking the average value one obtains

$$\begin{aligned}\langle \tau_{2y_1-1} T^t \tau_{2y_2-1} \rangle &= (1-\beta)\langle \tau_{2y_1-1} T^t \rangle \\ &= (1-\beta)\langle \tau_{2y_1-1} \rangle.\end{aligned}$$

We find

$$G(x_1, x_2; t) = \langle \eta_{x_1} \rangle \quad (x_1, x_2 \text{ odd}, \, x_1 \leq x_2 - 2 - 2t) \ . \tag{38}$$

Equations (37) and (38) are no surprise. The area defined by (37) and (38) is the exterior of the forward light cone of the particle at site x_2. If x_1 and x_2 are chosen in this way and both are in a region of uniform density (either in the bulk of the high-density phase or in the bulk of the low-density phase) one has $\eta_{x_1} = \eta_{x_2} = 1$ or 0, and therefore the connected correlation function $G_c(x_1, x_2; t)$ is time independent and 0 as one would expect. In the boundary region of the low-density phase where particles pile up and lead to a non-uniform density profile (or near the origin in the high-density phase) it is still time independent as it must be outside the light cone, but nonzero [see (32)]. This is due to the hard-core repulsion of the particles which behave as an incompressible liquid.

B. Correlation function on the edges of the light cone

On the right edge of the light cone of the particle at site x_2 defined by $x_1 = x_2 - 2 + 2t$ we can repeat the considerations that led to (37): All the parts on the rhs of (36) containing $\tau_{2y_2-1}\sigma_{2y_1-2t+2k} = \tau_{2y_1+1-2t}\sigma_{2y_1-2t+2k}$ with $k \geq 1$ vanish as a result of the fusion rules and only the first two parts in the sum remain. Although the term containing $\sigma_{2y_1-2t}\sigma_{2y_1+1-2t}\cdots\tau_{2y_1+1-2t}$ does not vanish due to fusion with τ_{2y_1+1-2t} it is nevertheless 0 since by definition $\sigma_{2y_1+1-2t}\tau_{2y_1+1-2t} = 0$. Therefore,

$$G(x_2 - 2 + 2t, x_2; t) = \langle \eta_{x_2} \rangle \quad (x_2 \text{ odd}) \ . \tag{39}$$

Consequently, the connected correlation function on the odd sublattice vanishes also on the forward edge of the light cone if the two points are in a region of uniform density. This is a result of the asymmetry of the model: if the system is in a region of uniform low density $\rho < 1/2$ the odd sublattice is empty and the vanishing of the correlator is trivial. In a region of uniform high density the even sublattice is completely occupied and particles on the odd sublattice effectively move only to the left (Fig. 4 in the Appendix) and are therefore uncorrelated to particles on the right edge of their (forward) light cone.

Due to the deterministic nature of the dynamics the particles on the odd sublattice move with the velocity of light, i.e., two lattice units per full time step as long as they are in a region of uniform high density. Thus we expect a singularity of the correlation function on the left edge of the light cone defined by $x_1 = x_2 - 2t$: Indeed, choosing $2y_2 - 1 = 2y_1 - 1 + 2t$ does not change the rhs of (36) since $\tau^2_{2y_1-1+2t} = \tau_{2y_1-1+2t}$ and therefore

$$\langle \tau_{2y_1-1} T^t \tau_{2y_1-1+2t} \rangle = \langle \tau_{2y_1-1} T^t \rangle = \langle \tau_{2y_1-1} \rangle.$$

For the correlator (34) we obtain

$$G(x_2 - 2t, x_2; t) = (1-\beta)^{-1}\langle \eta_{x_2-2t} \rangle \quad (x_2 \text{ odd}) \ . \tag{40}$$

Here the connected correlation function in a region of uniform high density does not vanish.

C. Correlation function inside the light cone

First, we note that in a region of uniform high density the result is again trivial. In such a region particles on the odd sublattice are found everywhere with equal probability (the equal-time connected two-point function is 0) and since they move with the velocity of light the time-dependent connected two-point function does also vanish.

If the profile is not uniform the calculation inside the light cone is nontrivial. With $x_1 = 2y_1 - 1$ as above and x_2 increasing beyond $2y_1 + 2 - 2t$ more and more contributions from the rhs of (36) are nonzero. We evaluated $G(x_1, x_2; t)$ for $t = 1, 2, 3$ inside the light cone on the computer (using the software system MATHEMATICA [14]) by calculating the exact form of (36) and then implementing the fusion rules (27) on the multipoint correlators on the rhs of (36). First we noticed that in a region of uniform high (low) density [all $\langle \eta_x \rangle$=1(0)] one obtains $G(x_1, x_2; t) = 1(0)$ and therefore $G_c(x_1, x_2; t) = 0$ as it should be. This observation is indeed a highly nontrivial test of the conjectured fusion rules (27) on which our calculation is based: Since Eqs. (27) are supposed to be exact, the result of the calculation of the time-dependent correlator must also be exactly 1 (0) if all η_x involved are set to 1 (0). Any other result would have shown that the fusion rules do not hold. Secondly, we observed that by taking $\alpha = 1-\beta$ the exact general form of the correlator becomes fairly obvious for arbitrary values of x_1, x_2, and t with x_1 inside the light cone of x_2. We found by generalizing our result from $t = 1,2,3$ to arbitrary t

$$G(x,x+2y;t) = \sum_{k=0}^{t+y-2}\left\{\binom{2t-2}{k}\beta^{2t-2-k}(1-\beta)^k\,[\beta\langle\,\eta_{x+3-2t+2k}\,\rangle + (1-\beta)\langle\,\eta_{x+4-2t+2k}\,\rangle]\right\} + \left[1-\sum_{k=0}^{t+y-2}\binom{2t-2}{k}\beta^{2t-2-k}(1-\beta)^k\right]\langle\,\eta_{x+2y}\,\rangle. \quad (41)$$

This is the main result of this section, valid for $t < (x-1)/2$ and $-t+2 \le y \le t-1$. The first restriction is due to boundary effects, and the second defines the interior of the light cone. In order to check this result we explicitly calculated $G(x,x+2y;t=4)$ on the computer for arbitrary α and β using (36) and the fusion rules and found it in exact agreement with our conjecture when setting $\alpha = 1-\beta$. As a second, independent test we set $\eta_x = 1$ (0) corresponding to the bulk value in the high-density region (low-density region) and indeed obtained $G_c(x_1,x_2;4) = 0$ for arbitrary α and β.

The choice $\alpha = 1-\beta$ is not too restrictive as far as the physics is concerned: since this curve runs across the phase diagram it covers both the high-density phase and the low-density phase and crosses the phase-transition line at $\alpha = \beta = 1/2$. In what follows we study $G(x_1,x_2;t)$ in the low-density phase along the curve $\beta = 1-\alpha > 1/2$ and on the phase-transition line at $\beta = 1/2$.

In the low-density phase we focus on the boundary region with a non-uniform density profile. For $\beta > 1/2$, $\alpha = 1-\beta$ the expression (23) for the density profile for large L gives $\langle\,\eta_{2x-1}\,\rangle = \langle\,\eta_{2x}\,\rangle = [(1-\beta)/\beta]^{L+2-2x}$ and therefore

$$\beta\langle\,\eta_{x+3-2t+2k}\,\rangle + (1-\beta)\langle\,\eta_{x+4-2t+2k}\,\rangle = \left(\tfrac{1-\beta}{\beta}\right)^{L+1-x+2t-2k}. \quad (42)$$

Inserting this into (41) and introducing the incomplete β function

$$\sum_{k=0}^{t+y-2}\binom{2t-2}{k}\beta^{2t-2-k}(1-\beta)^k = I_\beta(t-y,t+y-1) = 1 - I_{1-\beta}(t+y,t-y) - \binom{2t-2}{t-y-1}\beta^{t-y}(1-\beta)^{t+y-1}, \quad (43)$$

the correlation function (41) can conveniently be rewritten

$$G(x,x+2y;t) = \left(\tfrac{1-\beta}{\beta}\right)^{L-x}\left[I_{1-\beta}(t-y,t+y) + \left(\tfrac{\beta}{1-\beta}\right)^{2y-1} I_{1-\beta}(t+y,t-y)\right]. \quad (44)$$

For large times t (such that $|y|/t \ll 1$) the incomplete β function has the asymptotic form

$$I_{1-\beta}(t+y,t-y) = \begin{cases} \left(1-\dfrac{3}{4\xi_t}\right)\mathrm{e}^{1/\xi_t}\sqrt{\dfrac{\xi_t}{4\pi t}}\,\mathrm{e}^{-(y/\xi_r+t/\xi_t)}\,\mathrm{e}^{-y^2/t}, & \beta > \tfrac{1}{2} \\ P(\tfrac{y}{\sqrt{t}}) - \sqrt{\dfrac{t}{\pi\xi_t}}\,\mathrm{e}^{-y^2/t}, & \beta = \tfrac{1}{2} + (2\xi_t)^{-1/2} \end{cases} \quad (45)$$

with

$$\xi_t^{-1} = -\ln[4\beta(1-\beta)], \qquad \xi_r^{-1} = -\ln\tfrac{1-\beta}{\beta}\,. \quad (46)$$

and the probability integral

$$P(u) = 1/\sqrt{2\pi}\int_{-\infty}^{u}\exp(-t^2/2)dt.$$

In terms of ξ_t the inequality $\beta > 1/2$ in the upper expression of the rhs. of (45) has to be understood as $1 \ll \xi_t \lesssim t$. In the lower expression we assume $1 \ll t \lesssim \xi_t$. Note that the two length scales ξ_t and ξ_r are not independent quantities but related through $\xi_t^{-1} = \ln\cosh^2(\xi_r^{-1}/2)$. As β approaches 1/2, ξ_t and ξ_r diverge and are asymptotically related through $\xi_t \approx 4\xi_r^2$.

We define $\xi = \xi_r$ and $r = |y| = 1/2|x_2 - x_1|$ and insert (45) into (44). This gives the scaling form of the time-dependent correlation function in the scaling region of large $2\xi \lesssim t^{1/2}$,

$$G(x_1, x_2; t) = \mathrm{e}^{-R/\xi}\, \mathrm{e}^{-r/\xi} \sqrt{\frac{4\xi^2}{\pi t}}\, \mathrm{e}^{-t/(4\xi^2)}\, \mathrm{e}^{-r^2/t}, \quad (47)$$

where

$$R = \begin{cases} L + 1 - x_2 & \text{if } 2y = x_2 - x_1 > 0 \\ L + 1 - x_1 & \text{if } 2y = x_2 - x_1 < 0 \end{cases} \quad (48)$$

measures the distances of x_2 or x_1 from the boundary, depending on the sign of $x_2 - x_1$. $G(x_1, x_2; t)$ is invariant under the scaling transformation

$$R \to \lambda R, \quad r \to \lambda r, \quad \xi \to \lambda \xi, \quad t \to \lambda^2 t. \quad (49)$$

This is of the form corresponding to dynamical scaling with a dynamic critical exponent $z = 2$ and critical exponent $x = 0$.

If ξ increases beyond the crossover length scale $t^{1/2}$ the correlation function changes its form. At the critical point $\beta = 1/2$ we have $\langle \eta_x \rangle = x/L$ and up to corrections of order $1/L$ the exact expression (41) for the correlation function gives

$$G(x, x+2y; t) = \frac{x+2y}{L} - \frac{2t+2y}{L} I_{\frac{1}{2}}(t-y, t+y-1) + \frac{2}{L}\left(\frac{1}{2}\right)^{2t-2} \sum_{k=0}^{t+y-2} k \binom{2t-2}{k} . \quad (50)$$

Using

$$2 \sum_{k=0}^{t+y-2} k \binom{2t-2}{k} \beta^{2t-2-k}(1-\beta)^k = 2(1-\beta)(2t-2) I_\beta(t-y, t+y-1) - 2(t+y-1)\binom{2t-2}{t-y-1} \beta^{t-y}(1-\beta)^{t+y-1}, \quad (51)$$

and the expansion (45) of $I_{\frac{1}{2}}(t+y, t-y)$ we obtain with $2y = x_2 - x_1$ and $u = y/\sqrt{t}$,

$$G(x_1, x_2; t) = \frac{x_1 + x_2}{2L} - \frac{t}{L}\left(\frac{1}{2}\right)^{2t-2} \binom{2t-2}{t-y-1} - \frac{y}{L}\left[1 - 2 I_{\frac{1}{2}}(t-y, t+y)\right] \approx \frac{x_1+x_2}{2L} - \frac{\sqrt{t}}{\sqrt{\pi} L}\left[\mathrm{e}^{-u^2} + \sqrt{\pi} u (1 - 2P(u))\right]. \quad (52)$$

For finite distances y, t one has (up to corrections of order L^{-1} which we neglect) $x_1 = x_2 = x$ and the correlation function at the critical point is space and time independent with an amplitude x/L depending on the relative position of x in the bulk. For large times, $t \propto L$ and $y/t \ll 1$, the correlation function gets a contribution of order $L^{-1/2}$. $G(x_1, x_2; t)$ is invariant under the scale transformations (49) with the length scale ξ replaced by the size of the system L.

This result has a simple interpretation in terms of the constituent profiles discussed in the preceding section. For simplicity we consider $y = 0$. The operator $\eta_x T^t \eta_x$ gives 1 if x is in a region of high density both at times t_0 and $t_0 + t$. The probability that x is in the high-density region at time t_0 is x/L. This accounts for the constant x/L in (53). If we assume that the domain wall separating the low-density region from the high-density region performs a random walk of two lattice units per time step starting from its position x_0 at time t_0 then the resulting expectation value $\langle \eta_x T^t \eta_x \rangle$ will indeed be of the form (53).

VI. SUMMARY AND COMPARISON WITH OTHER EXCLUSION MODELS

Let us summarize our main results. We obtained recursion rules (14) which allow the construction of the steady state of the model defined by (1) and (2). Moreover we found for arbitrary values α and β of the injection and absorption rates exact steady-state expressions for the density profile (18), the current (19), the equal-time n-point density correlation function (30), and the time-dependent two-point function Eqs. (37)–(41). The expression (41) for the time-dependent two-point function inside the light cone was found only for $\alpha = 1 - \beta$.

We made the following observations:

(a) The phase diagram (Fig. 1) shows two phases. In the low-density phase ($\alpha < \beta$) the average density is $\rho = \alpha/2$ (in the limit $L \to \infty$) and in the high-density phase one has $\rho = 1 - \beta/2$. On the phase-transition line $\alpha = \beta$ the average density is $\rho = 1/2$.

(b) There is a shift in the average densities between the even sublattice and the odd sublattice [see Eqs. (24)–(26)]. This shift is the current j. In terms of the total average density ρ one finds $j = 2\rho$ in the low-density phase and $j = 2(1-\rho)$ in the high-density phase. On the phase-transition line ($\rho = 1/2$) the current is $j = \alpha$ [i.e. $j \neq 1 = 2\rho = 2(1-\rho)$].

(c) In the low-density phase the density profile decays on both sublattices to its respective bulk value exponentially with increasing distance from the boundary while in the high-density phase it increases exponentially to its respective bulk value with increasing distance from the origin. At the phase-transition line $\alpha = \beta$ the length scale ξ (23) associated with the exponential shape of the profile diverges and the profile increases linearly on both sublattices. The average density and the first derivatives of the current with respect to α and β have a discontinuity at the phase-transition line (in the thermodynamic limit $L \to \infty$).

(d) The decay length ξ is identical with the correlation length of the connected two-point density correlation function. Outside the light cone this correlator is of the scaling form $G(x_1, x_2; t = 0) = A r^\kappa \exp(-r/\xi)$ with exponent $\kappa = 0$. The amplitude A is space dependent as a result of breaking of the translational invariance (32) and (33).

(e) The time-dependent two-point correlation function $G(x_1, x_2; t)$ inside the light cone near the critical line (47) has a form compatible with dynamical scaling with dynamic critical exponent $z = 2$ and scaling dimension $x = 0$ [see the transformations (49)]. It contains the exponential $\exp(-r^2/t)$ characteristic for local dynamical scaling, but the amplitude is again space dependent due to breaking of the translational invariance. The correlation function changes its form when the correlation length increases beyond a crossover length scale of order $t^{1/2}$. On the critical line it becomes a space-dependent constant up to corrections of order L^{-1} if t is large but finite, and up to corrections of order $L^{-1/2}$ for times of order L.

(f) From an analysis of the two-point correlation function we found that the density profile can be considered as a superposition of step-function-type profiles with average density $\rho_1^{(\mathrm{even})} = \alpha$ and $\rho_1^{(\mathrm{odd})} = 0$ up to some point x_0 and average density $\rho_2^{(\mathrm{even})} = 1$ and $\rho_2^{(\mathrm{odd})} = 1 - \beta$ beyond this point up to the boundary. These densities are the sublattice densities in the low-density phase and high-density phase, respectively. The probability of finding the "domain wall" at site x_0 separating the two regions of high density and low density decreases exponentially with increasing distance from the boundary (origin) in the low-density (high-density) phase. On the phase-transition line this probability is space independent and the domain wall can be found everywhere with the same probability. Studying the time-dependent correlation function suggests that it performs a random walk around its position x_0 at time t_0.

We conclude our discussion of the deterministic *p-o* model with a brief comparison with other exclusion models and some conjectures for probabilistic exclusion models with parallel dynamics.

In the deterministic *p-p* model with a defect we found a phase diagram showing a low-density phase, a coexistence phase where a low-density region coexists with a high-density region and a high-density phase. The relation between the current and the sublattice densities and the total density discussed in (b) for the low- and high-density phases is identical with that in the *p-p* model in the respective phases. This is a consequence of the bulk dynamics which are identical in both cases and could have been guessed.

It is interesting to observe that there is also a correspondence between the coexistence phase of the *p-p* model and the phase-transition line here: In the *p-p* model with defect strength $1-q$ the quantity q is the hopping probability at a single link of the ring, say between sites L and 1, and therefore corresponds to an absorption of particles at site L and injection of particles at site 1 with rate q. This injection and absorption is correlated because of the particle number conservation. In the coexistence phase the current is density independent and one has $j = q$. In the *p-o* model on the phase-transition line discussed here particles are also injected and absorbed with the same rate α, but uncorrelated. The current is density independent, $j = \alpha$ as in the *p-p* model. The profile is built by constituent profiles with a region of low density up to some x_0 and a high-density region beyond that point. x_0 can be anywhere with the same probability. This suggests that also the profile in the coexistence phase of the *p-p* model with defect is built by such constituent profiles, with the distinction that there x_0 cannot be anywhere (because of particle number conservation) but the probability $p(x_0)$ of finding the domain wall is centered around some point R_0. We believe that similar phases occur also in probabilistic *p-p* models with a defect and in probabilistic *p-o* models. In such models particles do not always move if the neighboring site was empty as here but can stay with some nonzero probability even in the bulk. For mixed models (defect and some uncorrelated injection and absorption) we expect correspondingly a softening of the distribution $p(x_0)$.

All the features summarized under (c) (except the implied anisotropy between the even and odd sublattices) are in common with the phase transition from the low-density phase A_{I} to the high-density phase B_{I} in the *s-o* model [5]. This suggests that also the correlation functions are qualitatively the same (in the thermodynamic limit $L \to \infty$) near the phase-transition line. In the *s-o* model, however, the transition line $\alpha = \beta$ extends only up to $\alpha = \beta = 1/2$ as opposed to $\alpha = \beta = 1$ here. Correspondingly, in our model there is no maximal current phase with a power behavior of the density profile and no phases corresponding to the phases A_{II} or B_{II} (for $\alpha > 1/2$ or $\beta > 1/2$) of [5] where the shape of the density profile is determined by a product of a power-law behavior with an exponential decay.

We believe that phase transitions to such phases cannot occur in our model because of the deterministic nature of the dynamics. In [5] we argued that these phases result from an "overfeeding" of the system with particles: The system reaches its maximal transport capacity at density 1/2. In order to obtain average density 1/2 at the origin particles have to be injected with rate 1/2. If particles are injected at a higher rate they block each other rather than moving into the bulk and cause a phase transition. Here this cannot happen. The system reaches its maximal transport capacity also at average density 1/2 but here this corresponds to a completely filled even sublattice and an empty odd sublattice. An average density of 1 on the even sublattice at the origin can only occur if particles are injected at rate 1. Thus there can be no "overfeeding." The deterministic hopping rules imply that particles injected at the origin move away with velocity of light; therefore, there can be no mutual blockage near the origin. (Similar arguments can be used for a discussion of the dependence of the phase transitions on the absorption rate β by exchanging particles with holes and studying the injection of holes at the boundary.)

This discussion naturally leads to the conjecture that the probabilistic *p-o* model (which has not yet been studied) will have a phase diagram similar to that of the *s-o* model with a phase-transition line at $\alpha = \beta$ up to some value α_0 where the profile is constant on both sublattices and additional phase-transition lines at the values of α and β corresponding to an overfeeding of particles at the origin and holes at the boundary, respectively.

ACKNOWLEDGMENTS

It is a pleasure to thank E. Domany and D. Mukamel for interesting discussions. Financial support by the

Deutsche Forschungsgemeinschaft (DFG) is gratefully acknowledged.

APPENDIX: MAPPING TO A TWO-DIMENSIONAL VERTEX MODEL

Following the idea of Ref. [6] we want to show how the exclusion process defined by relations (1) and (2) is related to a two-dimensional vertex model. The discussion is partly similarly to that in [1] which we repeat for the convenience of the reader unfamiliar with this mapping. The mapping of the boundary conditions to vertices in the vertex model is different from [1].

Consider a four-vertex model on a diagonal square lattice defined as follows: Place an up- or down-pointing arrow on each link of the lattice and assign a nonzero Boltzmann weight to each of the vertices shown in Fig. 2. (All other configurations of arrows around an intersection of two lines, i.e., all other vertices, are forbidden in the bulk.) The partition function is the sum of the products of Boltzmann weights of a lattice configuration taken over all allowed configurations.

In the transfer-matrix formalism up- and down-pointing arrows in each row of a diagonal square lattice built by M of these vertices represent the state of the system at some given time t. Corresponding to the M vertices there are $L = 2M$ sites in each row represented by the links of the diagonal lattice. The configuration of arrows in the next row above (represented by the upper arrows of the same vertices) then corresponds to the state of the system at an intermediate time $t' = t + 1/2$, and the configuration after a full time step $t'' = t+1$ corresponds to the arrangement of arrows two rows above. Therefore each vertex represents a local transition from the state given by the lower two arrows of a vertex representing the configuration on sites j and $j+1$ at time t to the state defined by the upper two arrows representing the configuration at sites j and $j+1$ at time $t + 1/2$. The correspondence of the vertex language to the particle picture used in the Introduction can be understood by considering up-pointing arrows as particles occupying the respective sites of the chain while down-pointing arrows represent vacant sites, i.e., holes.

The diagonal-to-diagonal transfer matrix T acting on a chain of L sites (L even) of the vertex model with vertex weights $a_1, \ldots, c_1$ as shown in Fig. 2 is then defined by [1, 15]

$$T = \prod_{j=1}^{L/2} T_{2j-1} \prod_{j=1}^{L/2} T_{2j} = T^{\rm odd}\, T^{\rm even} \quad . \tag{A1}$$

The matrices T_j act nontrivially on sites j and $j+1$ in the chain; on all other sites they act as unit operator. All matrices T_j and $T_{j'}$ with $|j-j'| \neq 1$ commute. (The difference $j - j'$ is understood to be mod$L$.) For an explicit representation of the transfer matrix we choose a spin-1/2 tensor basis where the Pauli matrix σ_j^z acting on site j of the chain is diagonal and spin down at site j represents a particle (up-pointing arrow) and spin up a hole (down-pointing arrow). In this basis $\tau_j = \frac{1}{2}(1-\sigma_j^z)$ is the projection operator on particles on site j, $\sigma_j = \frac{1}{2}(1+\sigma_j^z)$ is the projector on holes, and $s_j^{\pm} = \frac{1}{2}(\sigma_j^x \pm i\sigma_j^y)$ ($\sigma^{x,y,z}$ being the Pauli matrices) create (s_j^-) and annihilate (s_j^+) particles, respectively.

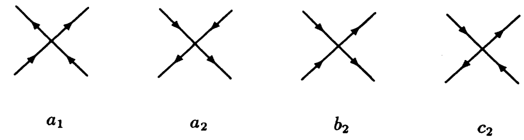

FIG. 2. Allowed bulk vertex configurations in the four-vertex model. Up-pointing arrows correspond to particles, down-pointing arrows represent vacant sites. In the dynamical interpretation of the model the Boltzmann weights give the transition probability of the state represented by the pair of arrows below the vertex to that above the vertex.

The bulk dynamics of our model is encoded in the transfer matrix by choosing the vertex weights as

$$a_1 = a_2 = b_2 = c_1 = 1. \tag{A2}$$

In the bulk this leads to

$$T_j = 1 + s_j^+ s_{j+1}^- - \tau_j \sigma_{j+1} = \begin{pmatrix} 1\,0\,0\,0 \\ 0\,1\,1\,0 \\ 0\,0\,0\,0 \\ 0\,0\,0\,1 \end{pmatrix}_{j,j+1} \quad . \tag{A3}$$

In the particle language the matrices T_j describe the local transition probabilities of particles moving from site j to site $j+1$ represented by the corresponding vertices. If sites j and $j+1$ are both empty or occupied, they remain as they are under the action of T_j. The same holds for a hole on site j and a particle on site $j+1$, corresponding to the diagonal elements of T_j, representing vertices a_1, a_2, and c_1. If there is a particle on site j and a hole on site $j+1$, the particle will move with probability one to site $j+1$. This accounts for vertex b_2.

As discussed in the Introduction we assume open boundary conditions with injection of particles on site 1 and absorption of particles on site L. This allows for the additional vertices shown in Fig. 3 together with vertex weights corresponding to the respective probabilities of creating and annihilating particles.

In a two-dimensional lattice (Fig. 4) we consider the half-vertices at the left boundary as the right arms of the vertices shown in Fig. 2 and Fig. 3 and the half-vertices at the right boundary as their left arms. Thus the left arrows define the particle configuration on site L and the right arrows are considered as site 1. Vertices a_1, a_2, and

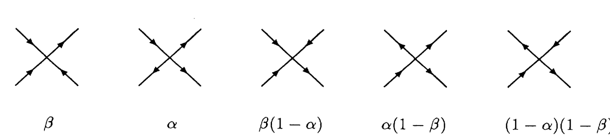

FIG. 3. Additional vertex configurations allowed at the boundary and their Boltzmann weights. The left arrows of these vertices describe the particle configuration at the boundary site L of the system while the right arrows define the particle configurations at the origin (site 1).

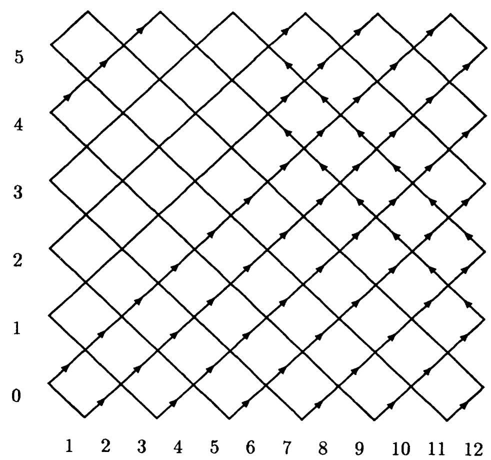

FIG. 4. Configuration of particles (up-pointing arrows) on a lattice of length $L = 12$ in space (horizontal) direction $M = 2t = 12$ between times $t = 0$ and $t = 5 + 1/2$ (vertical direction). Down-pointing arrows denoting vacant sites have been omitted from the drawing. At time $t = 0$ the even sublattice is filled and the odd sublattice empty. Particles are injected at site 1 after times $t = 0$ and $t = 4$. At the boundary (site 12) particles get stuck at times $t = 1$ and $t = 2$ and are absorbed at times $t = 0, 3, 4, 5$.

b_2 have a different weight at the boundary: $a_1' = 1 - \beta$, $a_2' = 1 - \alpha$, $b_2' = \alpha\beta$. Note that vertex b_2 at the boundary describes simultaneous absorption of a particle at site L and creation of a particle at site 1.

With this convention $T_L(\alpha, \beta)$ acting on sites L and 1 corresponding to the vertex weights shown in Fig. 3 is given by

$$\begin{aligned} T_L(\alpha,\beta) &= 1 + \alpha(s_1^- - \sigma_1) + \beta(s_L^+ - \tau_L) \\ &\quad + \alpha\beta(s_L^+ - \tau_L)(s_1^- - \sigma_1) \\ &= \begin{pmatrix} 1-\alpha & 0 & \beta(1-\alpha) & 0 \\ \alpha & 1 & \alpha\beta & \beta \\ 0 & 0 & (1-\alpha)(1-\beta) & 0 \\ 0 & 0 & \alpha(1-\beta) & 1-\beta \end{pmatrix}_{L,1} . \end{aligned} \tag{A4}$$

The transfer matrix $T = T(\alpha, \beta)$ acts parallel first on all even-odd pairs of sites $(2j, 2j+1)$ including the boundary pair $(L,1)$, then on all odd-even pairs. Thus in the first half time step T^{even} shifts particles from the even sublattice to the odd sublattice (so far it was not occupied) and then, in the second half step, T^{odd} moves particles from the odd sublattice to the even sublattice again. As a result, we expect an asymmetry in the average occupation of the even and odd sublattices which is related to the particle current. In a model with transfer matrix $\tilde{T} = T^{\text{odd}}T^{\text{even}}$ the asymmetry will be reversed, but there will be no essential difference in the physical properties of these two systems.

A possible configuration of particles in a 12x12 lattice is shown Fig. 4. Note that the presence of particles at site $x = 11$ and times $t = 2, 3$ imply the existence of particles on the left edge of their light cones as long as they move in a region where the even sublattice is fully occupied, i.e. they move with velocity of light (two lattice units per time step) to the left. A particle on an even lattice site at some (integer) time t always implies the existence of a particle on the right edge of its light cone up to the boundary.

The model has a particle-hole symmetry. We denote by $|x_1, x_2, \ldots, x_N\rangle = s_{x_1}^- s_{x_2}^- \ldots s_{x_N}^- |\ \rangle$ the N-particle state with particles on sites $x_1, \ldots, x_N$ ($|\ \rangle$ is the state with all spins up corresponding to no particle). The parity operator P reflects particles with respect to the center of the chain located between sites $x = L/2$ and $x = L/2 + 1$ and the charge conjugation operator $C = \prod_{j=1}^{L} \sigma_j^x$ interchanges particles and holes and therefore turns a N-particle state into a state with $L - N$ particles. One finds

$$(CP)\, T(\alpha, \beta)\, (CP) = T(\beta, \alpha) \ . \tag{A5}$$

In the bulk the particle current is conserved and can be obtained from the commutators of τ_{2x} and τ_{2x-1} with T. These relations play a crucial role in the construction of the steady state and the computation of the time-dependent correlation function. Defining the current operators j_{2x}^{even} and j_{2x-1}^{odd} by

$$\begin{aligned} j_{2x}^{\text{even}} &= \tau_{2x}\sigma_{2x+1} \quad (1 \le x \le L/2 - 1), \\ j_{2x-1}^{\text{odd}} &= (1 - \sigma_{2x-2}\sigma_{2x-1})(1 - \tau_{2x}\tau_{2x+1}) \\ &\qquad (2 \le x \le L/2 - 1), \end{aligned} \tag{A6}$$

a straightforward calculation yields ($x \ne L/2$):

$$\begin{aligned} [T, \tau_{2x-1}] &= T(\tau_{2x-1} - (1 - \sigma_{2x-2}\sigma_{2x-1})\tau_{2x}\tau_{2x+1}) \\ &= j_{2x-1}^{\text{odd}} - j_{2x-2}^{\text{even}}, \\ [T, \tau_{2x}] &= T(\sigma_{2x-2}\sigma_{2x-1}(1 - \tau_{2x}\tau_{2x+1}) - \sigma_{2x}) \\ &= j_{2x}^{\text{even}} - j_{2x-1}^{\text{odd}} \ . \end{aligned} \tag{A7}$$

Current conservation implies that the expectation values of the current operators j_{2x}^{even} and j_{2x-1}^{odd} do not depend on x, $\langle j_{2x}^{\text{even}} \rangle = \langle j_{2x-1}^{\text{odd}} \rangle = \text{const} = j$.

Note that the cases $\alpha, \beta = 0, 1$ are trivial. If $\alpha = 0$ no particles are injected and the steady state is $|\ \rangle$. If $\alpha = 1$ then in each time step a particle is injected and therefore the even sublattice fully occupied. Particles on the odd sublattice are randomly distributed with average density $1 - \beta$. As discussed above they move with velocity of light everywhere. Therefore the connected time-dependent two-point function on the odd sublattice is 0 except on the left edge of the (forward) light cone.

[1] G. Schütz, J. Stat. Phys. **71**, 485 (1993).
[2] J. Krug, Phys. Rev. Lett. **67**, 1882 (1991).
[3] S.A. Janowsky and J.L. Lebowitz, Phys. Rev. A **45**, 618 (1992).
[4] B. Derrida, E. Domany, and D. Mukamel, J. Stat. Phys. **69**, 667 (1992).
[5] G. Schütz and E. Domany, J. Stat. Phys. (to be published).

[6] D. Kandel, E. Domany, and B. Nienhuis, J. Phys. A **23**, L755 (1990).

[7] P. Meakin, P. Ramanlal, L.M. Sander, and R.C. Ball, Phys. Rev. A **34**, 5091 (1986); J. Krug and H. Spohn, in *Solids Far from Equilibrium: Growth, Morphology and Defects,* edited by C. Godreche (Cambridge University Press, Cambridge, 1991).

[8] M. Kardar, G. Parisi, and Y. Zhang, Phys. Rev. Lett. **56**, 889 (1986).

[9] L.-H. Gwa and H. Spohn, Phys. Rev. Lett. **68**, 725 (1992); Phys. Rev. A **46**, 844 (1992).

[10] B. Derrida and M.R. Evans, J. Phys. (Paris) (to be published); B. Derrida, M.R. Evans, V. Hakim, and V. Pasquier (unpublished).

[11] B.I. Halperin and P.C. Hohenberg, Phys. Rev. **177**, 952 (1992).

[12] J.L. Cardy, J. Phys. A **18**, 2771 (1985).

[13] M. Henkel, Int. J. Mod. Phys. C **3**, 1011 (1992).

[14] S. Wolfram, MATHEMATICA: *A System for Doing Mathematics by Computer* (Addison-Wesley, Redwood City, 1991).

[15] C. Destri and H.J. de Vega, Nucl. Phys. B **290**, 363 (1987).